

Fig. 3. Sun-illuminated multibeam bathymetry (illuminated from NE) showing (a) a probably older shipwreck (unknown age) with deep scours and long sediment drifts, (b) a shipwreck with minor scours, and (c) a more modern (20th century) shipwreck with small sediment drifts.

keeping the equipment running, and N. Anest and R. Lotti for preparing and analyzing hundreds of samples. We thank C. Bertinato, M. Cormier, R. Arko, and S. O'Hara for assistance in data processing and M. Turrin for essential administrative support. The benthic mapping project is managed by the Hudson River National Estuarine Research Reserve and

funded by the New York State Department of Environmental Conservation with funds from the Environmental Protection Fund through the Hudson River Estuary Program.

#### References

Bopp, R. E., S. N. Chillrud, E. L. Shuster, H. J. Simpson, and F. D. Estabrooks (1998), Trends in chlorinated hydrocar-

bon levels in Hudson River basin sediments, *Environ. Health Perspect.*, 106, suppl. 4, 1075–1079.  
Carbotte, S. M., R. E. Bell, W. B. F. Ryan, C. M. G. McHugh, A. Slagle, F. Nitsche, and J. Rubenstone (2004), Environmental change and oyster colonization within the Hudson River estuary linked to Holocene climate, *Geo Mar. Lett.*, 24, 212–224.  
McHugh, C. M. G., S. F. Pekar, N. Christie-Blick, W. B. F. Ryan, S. Carbotte, and R. Bell (2004), Spatial variations in a condensed interval between estuarine and open marine settings: Holocene Hudson River Estuary and adjacent continental shelf, *Geology*, 32, 169–172.  
Nitsche, F. O., R. Bell, S. M. Carbotte, W. B. F. Ryan, and R. Flood (2004), Process-related classification of acoustic data from the Hudson River Estuary, *Mar. Geol.*, 209, 131–145.

#### Author Information

F. O. Nitsche, R. Bell, S. M. Carbotte, W. B. F. Ryan, A. Slagle, S. Chillrud, and T. Kenna, Lamont-Doherty Earth Observatory of Columbia University, N.Y.; R. Flood, V. Ferrini, and R. Cerrato, Stony Brook University, State University of New York, Stony Brook; C. McHugh, Queens College, City University of New York, Flushing; and D. Strayer, Institute of Ecosystem Studies, N.Y.

## New Tools for Analyzing Time Series Relationships and Trends

PAGES 226, 232

Geophysical studies are plagued by short and noisy time series. These time series are typically nonstationary, contain various long-period quasi-periodic components, and have rather low signal-to-noise ratios and/or poor spatial sampling. Classic examples of these time series are tide gauge records, which are influenced by ocean and atmospheric circulation patterns, twentieth-century warming, and other long-term variability.

Remarkable progress recently has been made in the statistical analysis of time series. *Ghil et al.* [2002] presented a general review of several advanced statistical methods with a solid theoretical foundation. This present article highlights several new approaches that are easy to use and that may be of general interest.

Extracting trends from data is a key element of many geophysical studies; however, when the best fit is clearly not linear, it can be difficult to evaluate appropriate errors for the trend. Here, a method is suggested of finding a data-adaptive nonlinear trend and its error at any point along the trend. The method has significant advantages over, e.g., low-pass filtering or fitting by polynomial functions in that as the fit is data adaptive, no preconceived functions are forced on the data; the errors associated with the trend are then usually much smaller than individual measurement errors.

Fourier or wavelet techniques are often used in time series analysis extracting periodic signals. However, a difficulty for many users has

been how to relate the wavelet spectrum they compute with another spectrum from a different series, in order to examine causality and phase relations expected in an a priori mechanism.

*Grinsted et al.* [2004] present two new techniques that advance the wavelet approach popularized by *Torrence and Compo* [1998]. Often, it is not simply the wavelet spectrum of a time series that is of interest, but rather the similarity it has with the spectrum from another, putatively related series. Two suitable methods to examine the relationship between two spectra are the cross wavelet transform (XWT) and wavelet transform coherence (WTC). *Torrence and Compo* [1998] discuss both, but provide no software.

*Grinsted et al.* [2004] give this software and additionally formulate statistical significance tests. XWT exposes regions in time-frequency space with high common power, and further reveals information about the phase relationship between the two series. If the two series are physically related, a consistent or slowly varying phase lag would be expected that can be tested against mechanistic models of the physical process.

WTC can be thought of as the local correlation between the time series in time-frequency space. Where XWT unveils high common power, WTC finds locally phase locked behavior. The more desirable features of the WTC come at the price of being slightly less localized in time-frequency space.

The significance level of the WTC has to be determined using Monte Carlo methods. The XWT significance level can be tested analytically against red noise (which, unlike white noise, is autocorrelated, and hence can mimic long-term

trends) using the first-order autoregressive coefficient of the time series. The WTC and XWT methods are useful especially in nonstationary time series where there may be statistically significant periods of correlation for only certain intervals of the whole record.

It is advisable to have a good understanding of the data before starting wavelet analyses; the time series, for example, should be close to normally distributed. If the time series is not, then it should be transformed. Consider what outcomes are expected given the proposed linking mechanism. It is cautioned against blindly applying these methods to randomly chosen data sets.

#### ENSO and Temperatures in England

An example of the XWT and WTC methods can be seen in Figure 1, which shows part of the 340-year-long central England temperature (CET) series [e.g., *Plaut et al.*, 1995] that overlaps with the atmospheric representation of El Niño–Southern Oscillation (ENSO), the Southern Oscillation Index (SOI). Both series exhibit strong power in the 4- to 8-year period band. However, here, a 14-year cycle that *Plaut et al.* [1995] find clearly in the full CET is discussed. *Jevrejeva et al.* [2004] also found a 13.9-year periodicity SOI signal that is transmitted, with a 1.8- to 2.1-year lag, by equatorial coupled waves and fast boundary waves to the polar regions.

To test whether the CET is also recording this signal, the XWT and WTC plots were examined; indeed, there is a peak of power and coherence around the 14-year period. However, the phase varies considerably over the time series, suggesting that the mechanism must have changed appreciably—or alternatively, that there is no cause and effect mechanism involved and the coincident power is merely accidental.

The authors believe that there is most likely a causative relationship but that atmospheric

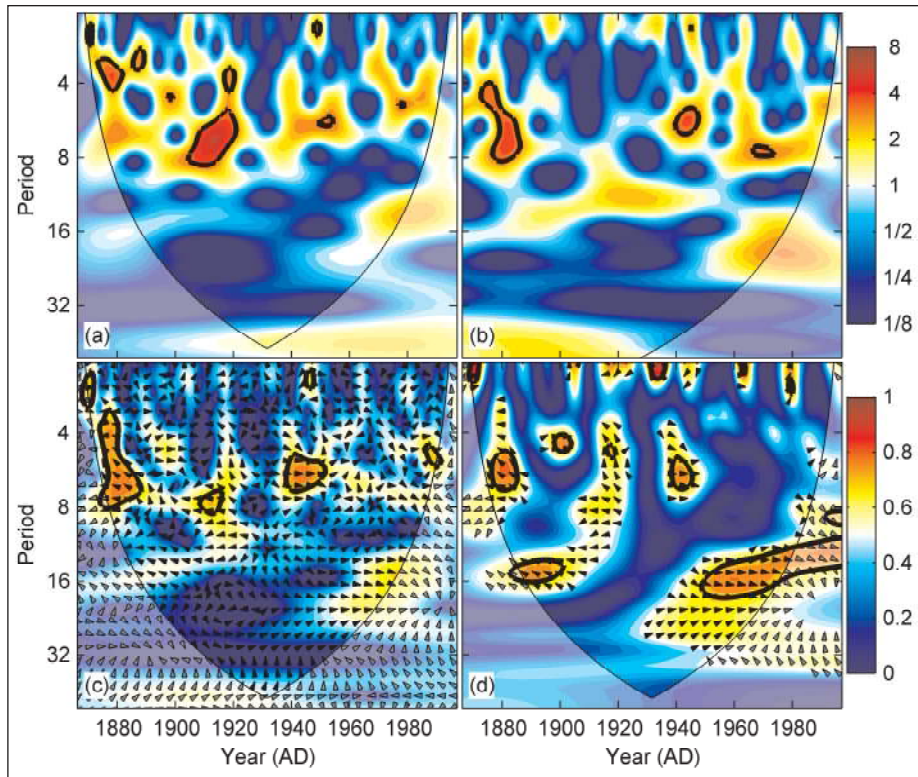


Fig. 1. The wavelet spectra of the SOI (a) and CET (b) series and their XWT (c), upper colorbar representing normalized variances and their WTC (d), lower colorbar - units are wavelet squared coherencies. The vectors indicate the phase difference (an arrow pointing from left to right signifies in-phase, and an arrow pointing upward means that CET lags SOI by  $90^\circ$  (i.e., the phase angle is  $270^\circ$ ); the dimmed plot area is affected by data boundaries. Bold contours are 95% confidence levels.

conditions around the 1920s were in a transitional state, with, for example, the North Atlantic Oscillation and the Arctic Oscillation and Scandinavian surface air temperatures all being rather uncorrelated for that period [e.g., Jevrejeva et al., 2003].

*Nonlinear Trends in Sea Level and Temperature*

The widely used methods of estimating trends are simple linear or polynomial least squares fitting, or low-pass filtering of data followed by extension to data set boundaries by some method [e.g., Mann, 2004]. A new approach makes use of singular spectrum analysis (SSA) [Ghil et al., 2002] to extract a nonlinear trend and, in addition, to find the confidence interval of the nonlinear trend. This gives confidence intervals that are easily calculated and much smaller than for polynomial fitting.

Monte Carlo SSA (MC-SSA) [Allen and Smith, 1996] is used to decompose the time series with data-adaptive orthogonal filters. SSA amplifies signal-to-noise ratio by separating the original time series into low-frequency trends and narrow-band quasi-periodic signals, with the rest (assumed to be noise) distributed among the filters.

In MC-SSA, lagged copies of the time series are used to define coordinates in a phase space that will approximate the dynamics of the system. It is often suggested that the number of lagged copies (or the embedding

dimension) is chosen between one fifth and one half the length of the time series, reflecting a trade-off between spectral resolution and optimal noise reduction. The smaller the embedding space, the shorter the length of the window over which the resolved components are calculated, and the less resolved is each component. The longer the window, the greater the frequency resolution of each component, but the greater the chance that noise is mistaken for signal and that a greater proportion of the time series is affected by the data boundaries.

A wise choice of embedding dimension can be made with a priori insight or perhaps more commonly may be found by simply playing with the data. The trend is the collection of reconstructed components that have a periodicity longer than about twice the length of the time window (or embedding dimension).

The amount of measurement noise remaining in the trend can be estimated by generating a large surrogate set of white measurement noise added to the original time series and then convoluting with the SSA filter representing the trend. Doing so allows one to specify uncertainties in the predictions where the SSA filter overlaps data boundaries. Here, the series is padded so the local trend is preserved (cf. minimum roughness criterion, [Mann, 2004]). The confidence interval of the nonlinear trend is usually much smaller than for a least squares fit, as the data are not forced to fit any specified set of basis functions.

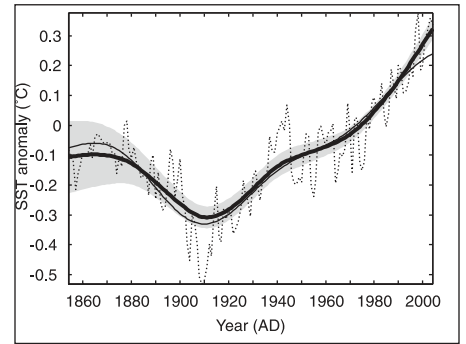


Fig. 2. Nonlinear trend in global ( $60^\circ\text{S}-60^\circ\text{N}$ ) sea surface temperature anomaly relative to 1961–1990 (bold curve) based on the 150-year-long reconstructed sea surface temperature  $2^\circ$  data set (dotted [Smith and Reynolds, 2004]), using an embedding dimension equivalent to 30 years; errors are the mean yearly standard errors of the data set. Shading is the 95% confidence interval of the nonlinear trend. The curve was extended to the data boundaries using a variation on the minimum roughness criterion [Mann, 2004]. For comparison, the thin curve is the low-pass trend using Mann's low-pass filter and minimum roughness with a 60-year cutoff frequency.

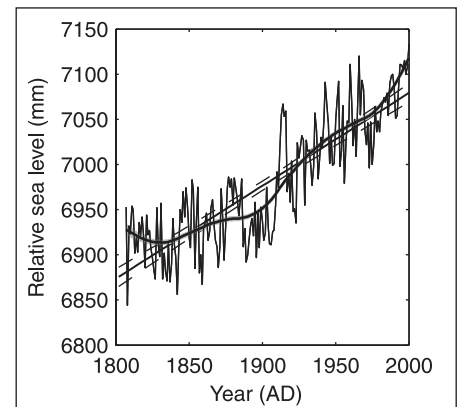


Fig. 3. Nonlinear and linear trends in time series of mean sea level at Brest, France, for an embedding dimension equivalent to 30 years and an individual measurement standard error of 10 mm. The 95% confidence interval for the nonlinear fit is shaded and marked by the curved lines for the linear fit.

Figure 2 illustrates how the nonlinear trend fits the global sea surface temperature data set. Note the increased size of the confidence interval in the early part of the record due to larger observational errors at that time, and the poor quality that a linear fit would provide.

Figure 3 shows the linear and nonlinear trends for sea level at Brest, France, one of the world's longest sea level records. Note the small confidence intervals of the nonlinear compared with the linear fits. To date, linear fits have usually been used to estimate sea level rise despite the clear inconsistency of the data to a linear model. The nonlinear trend shows a more rapid rise around 1920–1940 than at present and a slight decreasing of sea level prior to 1840 that is not detected by the linear trend. A comparison with Figure 2 shows that there is not a simple correlation

between global sea surface temperatures and sea level at any particular place.

#### Acknowledgments

We thank the Natural Environmental Research Council, UK, the Academy of Finland and Thule Institute, Finland for financial support.

#### References

Allen, M. R., and L. A. Smith (1996), Monte Carlo SSA: Detecting irregular oscillations in the presence of coloured noise, *J. Clim.*, **9**, 3373–3404.  
Ghil, M., et al. (2002), Advanced spectral methods for climatic time series, *Rev. Geophys.*, **40**(1), 1003, doi:10.1029/2000RG000092.

Grinsted, A., J. C. Moore, and S. Jevrejeva (2004), Application of the cross wavelet transform and wavelet coherence to geophysical time series, *Nonlinear Processes Geophys.*, **11**, 561–566. (Available at <http://www.pol.ac.uk/home/research/waveletcoherence/>)  
Jevrejeva, S., J. C. Moore, and A. Grinsted (2003), Influence of the Arctic Oscillation and El Niño–Southern Oscillation (ENSO) on ice conditions in the Baltic Sea: The wavelet approach, *J. Geophys. Res.*, **108**(D21), doi:10.1029/2003JD003417.  
Jevrejeva, S., J. C. Moore, and A. Grinsted (2004), Oceanic and atmospheric transport of multiyear El Niño–Southern Oscillation (ENSO) signatures to the polar regions, *Geophys. Res. Lett.*, **31**, L24210, doi:10.1029/2004GL020871.  
Mann, M. (2004), On smoothing potentially nonstationary climate time series, *Geophys. Res. Lett.*, **31**, L07214, doi:10.1029/2004GL019569.

Plaut, G., M. Ghil, and R. Vautard (1995), Interannual and interdecadal variability in 335 years of central England temperatures, *Science*, **268**, 710–713.  
Smith, T. M., and R. W. Reynolds (2004), Improved extended reconstruction of SST (1854–1997), *J. Clim.*, **17**, 2466–2477.  
Torrence, C., and G. P. Compo (1998), A practical guide to wavelet analysis, *Bull. Am. Meteorol. Soc.*, **79**, 61–78. (Available at <http://paos.colorado.edu/research/wavelets/>)

#### Author Information

J. C. Moore and A. Grinsted, Arctic Centre, University of Lapland, Rovaniemi, Finland; and S. Jevrejeva, Proudman Oceanographic Laboratory, Liverpool, U.K.

# NEWS

## Hotspot Ecosystem Research on the Margins of European Seas

PAGE 226

The European Union has recently funded an integrated project called Hotspot Ecosystem Research on the Margins of European Seas, or HERMES, which began on 1 April 2005 and will run for four years. HERMES is designed to gain new insights into the biodiversity, structure, function, and dynamics of ecosystems along Europe's deep-ocean margin.

It represents the first major attempt to understand European deepwater ecosystems and their environments in an integrated way, by bringing together expertise in biodiversity, geology, sedimentology, physical oceanography, microbiology, and biogeochemistry, so that the relationship between biodiversity and ecosystem functioning can be understood. The project extends beyond basic research, mapping, and habitat classification into ecosystem modeling and policy advice. The modeling is aimed at improving the ability to forecast the effect on ecosystems of natural and anthropogenic perturbations.

Finally, an attempt will be made to integrate the scientific output of the project with socioeconomics and legal research to underpin the development of a comprehensive European Ocean and Seas Governance strategy (see [http://europa.eu.int/comm/fisheries/news\\_corner/discours/speech55\\_en.htm](http://europa.eu.int/comm/fisheries/news_corner/discours/speech55_en.htm)). This will be the first time that such an integrated approach has been adopted on a pan-European scale for the deep sea. The intended outcome is to develop concepts and strategies for the sustainable use of offshore marine resources, while taking into account the negative impact of human activities.

The primary ecosystems to be studied include biodiversity hot spots, such as cold seeps, cold-water coral mounds, canyons, and

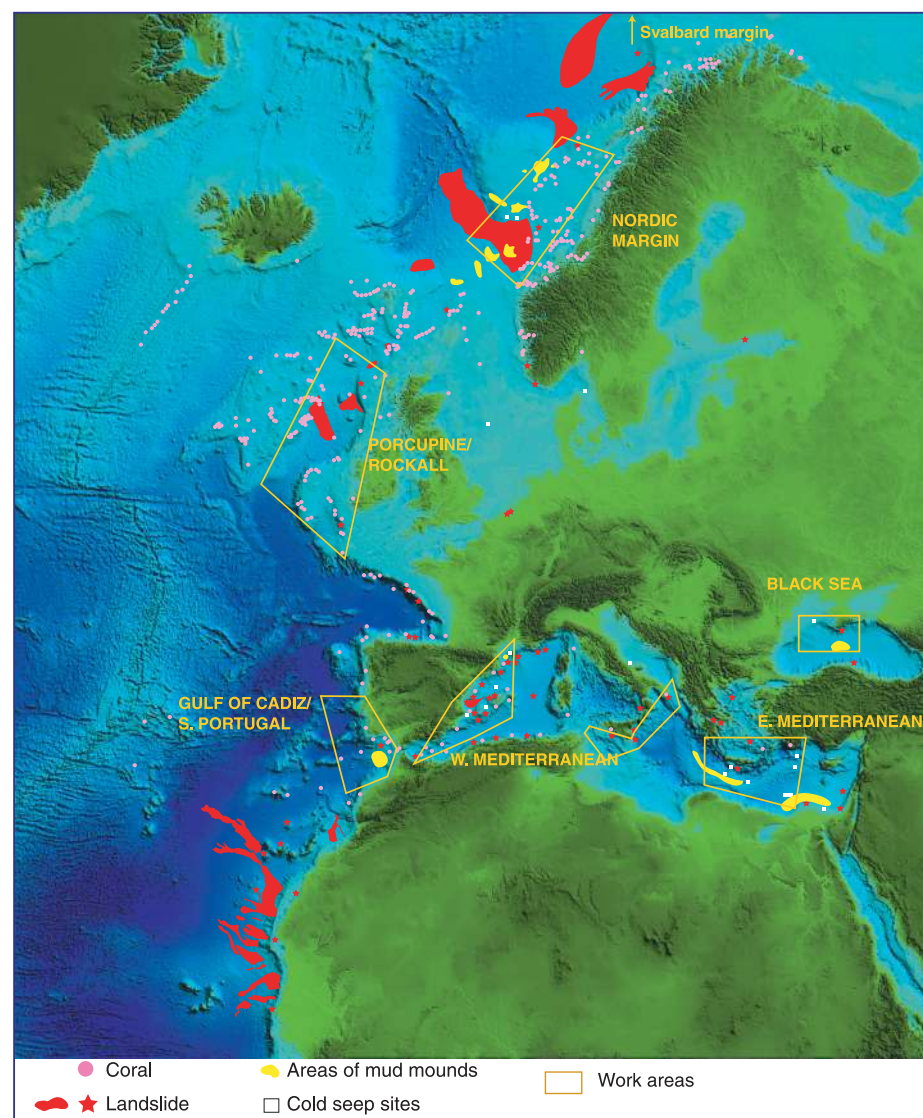


Fig. 1. Bathymetry of the European margin and the distribution of canyons, overlain by known occurrences of cold-water corals, cold seeps, and mud volcanoes. Irregular red areas show the locations of major landslides. Yellow boxes indicate HERMES study sites.

anoxic environments, where the geosphere and hydrosphere influence the biosphere through the escape of fluids, presence of gas hydrates, and deepwater currents. Open-slope environments, where landslides and deep-ocean circulation affect ecosystem development, will also be studied. These

systems require urgent study because of their possible biological fragility, unique genetic resources, global relevance to carbon cycling, and possible susceptibility to global change and man-made disturbances. Past changes, including catastrophic events, will be assessed using sediment archives. HERMES will make